

Article

Monoterpenoid Glycosides from the Leaves of *Ligustrum robustum* and Their Bioactivities

Shi-Hui Lu ^{1,*}, Jing Huang ^{2,*}, Hao-Jiang Zuo ³, Zhong-Bo Zhou ¹, Cai-Yan Yang ¹ and Zu-Liang Huang ^{1,*}

¹ College of Pharmacy, Youjiang Medical University for Nationalities, Baise 533000, China; zzb7855@163.com (Z.-B.Z.); yjsyangcaiyan@163.com (C.-Y.Y.)

² Key Laboratory of Drug Targeting, Ministry of Education, West China School of Pharmacy, Sichuan University, Chengdu 610041, China

³ Department of Laboratory Science of Public Health, West China School of Public Health, Sichuan University, Chengdu 610041, China; zuohaojiang@scu.edu.cn

* Correspondence: lushihui0818@126.com (S.-H.L.); huangj_pharm@scu.edu.cn (J.H.); ymhzl0416@163.com (Z.-L.H.)

† These authors contributed equally to this article.

Abstract: The leaves of *Ligustrum robustum* have been applied as Ku-Ding-Cha, a functional tea to clear heat, remove toxins, and treat obesity and diabetes, in Southwest China. The phytochemical research on the leaves of *L. robustum* led to the isolation and identification of eight new monoterpenoid glycosides (1–8) and three known monoterpenoid glycosides (9–11). Compounds 1–11 were tested for the inhibitory activities on fatty acid synthase (FAS), α -glucosidase, α -amylase, and the antioxidant effects. Compound 2 showed stronger FAS inhibitory activity (IC_{50} : $2.36 \pm 0.10 \mu M$) than the positive control orlistat (IC_{50} : $4.46 \pm 0.13 \mu M$), while compounds 1, 2, 5 and 11 displayed more potent ABTS radical scavenging activity (IC_{50} : 6.91 ± 0.10 – $9.41 \pm 0.22 \mu M$) than the positive control L-(+)-ascorbic acid (IC_{50} : $10.06 \pm 0.19 \mu M$). This study provided a theoretical basis for the leaves of *L. robustum* as a functional tea to treat obesity.

Keywords: *Ligustrum robustum*; monoterpenoid glycoside; FAS; α -glucosidase; antioxidant; anti-obesity; hypoglycemic



Citation: Lu, S.-H.; Huang, J.; Zuo, H.-J.; Zhou, Z.-B.; Yang, C.-Y.; Huang, Z.-L. Monoterpenoid Glycosides from the Leaves of *Ligustrum robustum* and Their Bioactivities. *Molecules* **2022**, *27*, 3709. <https://doi.org/10.3390/molecules27123709>

Academic Editor: Kyoko Nakagawa-Goto

Received: 8 May 2022

Accepted: 7 June 2022

Published: 9 June 2022

Publisher's Note: MDPI stays neutral with regard to jurisdictional claims in published maps and institutional affiliations.



Copyright: © 2022 by the authors. Licensee MDPI, Basel, Switzerland. This article is an open access article distributed under the terms and conditions of the Creative Commons Attribution (CC BY) license (<https://creativecommons.org/licenses/by/4.0/>).

1. Introduction

Ku-Ding-Cha has been used widely as a functional tea to clear heat, remove toxins, and treat obesity, diabetes and so on, in Southwest China for a long time [1,2]. It was produced from the leaves of more than 30 plants from 13 genera in 12 families, in which the most common categories were from the genus *Ligustrum* (Oleaceae) and the genus *Ilex* (Aquifoliaceae) [3]. *Ligustrum robustum* (Roxb.) Blume, distributed widely in Southwest China, India, Burma, Vietnam and Cambodia, has been consumed as Ku-Ding-Cha in Southwest China, especially in Guizhou Province [4]. *L. robustum* has been classified as a food by the Chinese Ministry of Health since 2011 [5]. In the past two decades, the phytochemical studies on *L. robustum* led to the isolation and identification of monoterpenoid glycosides, phenylethanoid glycosides, iridoid glycosides, flavonoid glycosides and triterpenoids [1,6–11]. The biological research on *L. robustum* reported the anti-obesity activity of the total glycosides and the aqueous extract [2,5], the antioxidative, anti-inflammatory and hepato-protective effects of the aqueous extract [4], and the antioxidant effect of some constituents [1,10]. In our previous study on *L. robustum* [12], some antioxidative and α -glucosidase inhibitory components, which might be a part of anti-diabetic ingredients of *L. robustum* [13–16], were discovered. However, to the best of our knowledge, the exact anti-obesity ingredients of *L. robustum* and their mechanisms are still unclear so far.

Studies revealed that fatty acid synthase (FAS) catalyzed the synthesis of saturated long-chain fatty acids from acetyl-coenzyme A, malonyl-CoA and NADPH; FAS expressed

high in normal adipose, liver tissues, lactating mammary glands, and in patient tumor tissues at later stages of disease, while most normal tissues showed low levels of FAS expression [17–19]. Thus, FAS is a potential therapeutic target for anti-obesity and anti-cancer drugs. There have been no reports on the screening FAS inhibitors from the constituents of *L. robustum*. In this work, eight new monoterpenoid glycosides, named ligurobustosides T (1), T₁ (2), T₂ (3), T₃₋₄ (4), T₅ (5), T₆ (6), T₇ (7), T₈₋₉ (8), and three known monoterpenoid glycosides (9–11) (Figure 1) were isolated from the leaves of *L. robustum*. This paper deals with the isolation and structure elucidation of 1–11, and it describes their inhibitory activities on FAS, α -glucosidase, α -amylase, and their antioxidant effects.

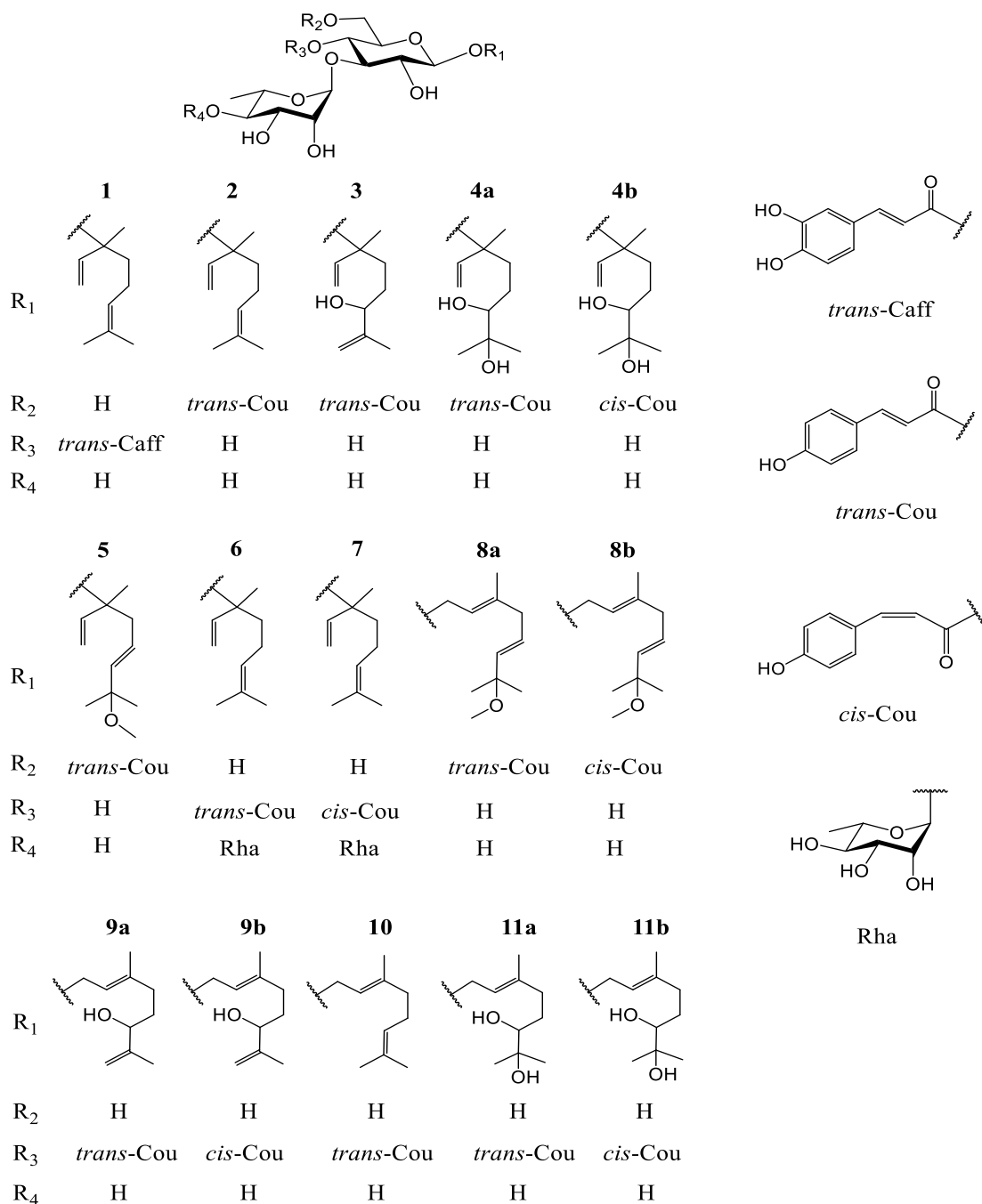


Figure 1. Structures of compounds 1–11 from the leaves of *L. robustum*.

2. Material and Methods

2.1. General Experimental Procedure

First, 1D and 2D NMR spectra were measured on a Bruker Ascend™ 400 NMR spectrometer (Bruker, Germany) (^1H at 400 MHz, ^{13}C at 100 MHz) or an Agilent 600/54 Premium Compact NMR spectrometer (Agilent, Santa Clara, CA, USA) (^1H at 600 MHz, ^{13}C at 150 MHz) with CD_3OD as the solvent at 25 °C. Chemical shifts are expressed in δ (ppm) with tetramethylsilane (TMS) as the internal standard, and coupling constants (J) are reported in Hz. High-resolution electrospray ionization mass spectroscopy (HRESIMS) was carried out on a Waters Q-TOF Premier mass spectrometer (Waters, Milford, MA, USA). The IR absorption spectrum was measured with a PerkinElmer Spectrum Two FT-IR spectrometer (PerkinElmer, Waltham, MA, USA). UV spectrum was recorded using a UV2700 spectrophotometer (Shimadzu, Kyoto, Japan). Optical rotation value was analyzed with an AUTOPOL VI automatic polarimeter (Rudolph, Hackettstown, NJ, USA).

UV-vis absorbance was analyzed with a Spark 10M microplate reader (Tecan Trading Co. Ltd., Shanghai, China). Preparative HPLC was performed on a GL3000-300 mL system instrument (Chengdu Gelai Precision Instruments Co., Ltd., Chengdu, China) with a GL C-18 column (particle size 5 μm , 50 \times 450 mm) and a UV-3292 detector operating at 215 nm, eluting with MeOH- H_2O at a flow rate of 30 mL/min. Column chromatography (CC) was performed on silica gel (SiO_2 : 200–300 mesh, Qingdao Ocean Chemical Industry Co., Qingdao, China), MCI-gel CHP-20P (75–150 μm , Mitsubishi Chemical Co., Tokyo, Japan), and polyamide (60–90 mesh, Jiangsu Changfeng Chemical Industry Co., Yangzhou, China). TLC was carried out on precoated HPTLC Fertigplatten Kieselgel 60 F₂₅₄ plates (Merck), and the spots were visualized by spraying with α -naphthol-sulfuric acid solution or 10% sulfuric acid ethanolic solution and heating at 105 °C for 2–5 min. NADPH and acetyl-coenzyme A (Ac-CoA) were obtained from Zeye Biochemical Co., Ltd. (Shanghai, China). Methylmalonyl coenzyme A tetralithium salt hydrate (Mal-CoA) was purchased from Sigma-Aldrich (St. Louis, MO, USA). 2,2-Diphenyl-1-picrylhydrazyl (DPPH) was obtained from Macklin Biochemical Co., Ltd. (Shanghai, China). 2,2'-Azino-bis(3-ethylbenzthiazoline-6-sulphonic acid) ammonium salt (ABTS) was purchased from Aladdin Industrial Co., Ltd. (Shanghai, China).

2.2. Plant Material

The leaves of *L. robustum* were collected from Yibin City, Sichuan Province, China, in April 2017, and identified by Professor Guo-Min Liu (Kudingcha Research Institute, Hainan University, Haikou, 570228, China). A voucher specimen (No. 2017041sh) was deposited in West China School of Pharmacy, Sichuan University, China.

2.3. Extraction and Isolation

The fresh leaves of *L. robustum* were stirred and dried at 120 °C for 50 min and then powdered. The dried raw powder (7.0 kg) was extracted under reflux with 70% ethanol (28 L \times 1) in a multi-function extractor for 2 h. The ethanol extract was filtrated and concentrated in vacuo to obtain a dark brown paste (2.2 kg). The paste was dissolved in 95% ethanol (3 L), and then, the distilled water (3 L) was added to precipitate the chlorophyll. After filtration, the filtrate was concentrated in vacuo to gain a brown residue (1.0 kg). The residue was chromatographed on silica gel column, eluting with CH_2Cl_2 -MeOH (10:0–0:10), to yield Fr. I (84 g), Fr. II (145 g), Fr. III (93 g), and Fr. IV (70 g). Fr. II was separated repeatedly by CC on silica gel, eluting with CH_2Cl_2 -MeOH- H_2O (200:10:1–40:10:1) or EtOAc-MeOH- H_2O (50:2:1–50:3:1), and then subjected to polyamide column (EtOH- H_2O , 0:10–7:3) and MCI column (MeOH- H_2O , 3:7–7:3), and purified finally by preparative HPLC (MeOH- H_2O , 40:60–65:35) or silica gel column (EtOAc- MeOH- H_2O , 50:2:1–50:3:1), to yield **1** (48.5 mg), **2** (49.2 mg), **3** (11.8 mg), **4** (15.3 mg), **5** (8.2 mg), **6** (17.6 mg), **7** (8.2 mg), **8** (10.7 mg), **9** (20.0 mg), **10** (135.8 mg) and **11** (38.6 mg).

Compound **1**: yellowish amorphous powder. $[\alpha]_{\text{D}}^{20}$ -91.9 (c 0.27, MeOH); UV (MeOH) λ_{max} : (log ϵ) 214 (4.2), 244 (4.1), 331 (4.4) nm; IR (film) ν_{max} : 3375, 2923, 1694, 1630, 1601,

1515, 1446, 1376, 1261, 1025, 928, 836, 811 cm^{-1} ; ^1H NMR (CD_3OD , 400 MHz) data, see Table 1; ^{13}C NMR (CD_3OD , 100 MHz) data, see Table 2; HRESIMS m/z 647.2679 $[\text{M} + \text{Na}]^+$ (calculated for $\text{C}_{31}\text{H}_{44}\text{NaO}_{13}$, 647.2680).

Compound 2: white amorphous powder. $[\alpha]_D^{23}$ -29.9 (c 0.98, MeOH); UV (MeOH) λ_{max} ($\log \epsilon$): 209 (3.9), 230 (3.9), 314 (4.4) nm; IR (film) ν_{max} : 3375, 2927, 1689, 1632, 1604, 1515, 1445, 1263, 1169, 1037, 832 cm^{-1} ; ^1H NMR (CD_3OD , 400 MHz) data, see Table 1; ^{13}C NMR (CD_3OD , 100 MHz) data, see Table 2; HRESIMS m/z 631.2728 $[\text{M} + \text{Na}]^+$ (calculated for $\text{C}_{31}\text{H}_{44}\text{NaO}_{12}$, 631.2730).

Compound 3: white amorphous powder. $[\alpha]_D^{25}$ -11.0 (c 0.47, MeOH); UV (MeOH) λ_{max} ($\log \epsilon$): 208 (3.9), 230 (3.9), 316 (4.4) nm; IR (film) ν_{max} : 3370, 2926, 2855, 1696, 1605, 1514, 1448, 1262, 1169, 1036, 833 cm^{-1} ; ^1H NMR (CD_3OD , 600 MHz) data, see Table 1; ^{13}C NMR (CD_3OD , 100 MHz) data, see Table 2; HRESIMS m/z 647.2680 $[\text{M} + \text{Na}]^+$ (calculated for $\text{C}_{31}\text{H}_{44}\text{NaO}_{13}$, 647.2680).

Table 1. ^1H NMR data of compounds 1–8 from *L. robustum* in CD_3OD ^a.

No	1 ^b	2 ^b	3 ^c	4a ^b	4b ^b
1	5.22 dd (10.8, 1.2) 5.26 dd (17.6, 1.2)	5.19 dd (10.8, 1.2) 5.23 dd (18.0, 1.2)	5.19 br. d (10.8) 5.24 br. d (18.0)	5.19 dd (10.8, 2.0) 5.24 dd (18.0, 2.0)	5.19 dd (10.8, 2.0) 5.24 dd (18.0, 2.0)
2	5.93 dd (17.6, 10.8)	5.90 dd (18.0, 10.8)	5.90 dd (18.0, 10.8)	5.92 dd (18.0, 10.8)	5.92 dd (18.0, 10.8)
4	1.58 m 1.62 m	1.56 m 1.60 m	1.22 dd (10.8, 2.4)	1.57 m 1.90 m	1.57 m 1.90 m
5	2.04 m	2.02 m	1.60 m	1.32 m 1.70 m	1.32 m 1.70 m
6	5.10 tt (7.2, 1.6)	5.07 tt (7.2, 1.2)	3.95 m	3.21 dd (10.4, 2.0)	3.21 dd (10.4, 2.0)
8	1.67 s	1.62 br. s	4.78 br. s 4.88 br. s	1.11 s	1.11 s
9	1.60 s	1.56 br. s	1.67 s	1.14 s	1.14 s
10	1.39 s	1.34 s	1.35 s	1.36 s	1.36 s
7-OCH ₃					
Glc					
1'	4.43 d (8.0)	4.39 d (8.0)	4.38 d (8.4)	4.41 d (8.0)	4.36 d (8.0)
2'	3.36 m	3.29 m	3.29 m	3.29 m	3.27 m
3'	3.77 t (9.2)	3.49 m	3.48 m	3.50 t (8.8)	3.46 t (8.8)
4'	4.89 m	3.34 m	3.32 m	3.33 m	3.29 m
5'	3.45 m	3.49 m	3.48 m	3.47 m	3.42 m
6'	3.49 m 3.57 m	4.30 dd (12.0, 6.8) 4.45 dd (12.0, 2.4)	4.30 dd (12.0, 6.6) 4.45 dd (12.0, 2.4)	4.30 dd (12.0, 6.0) 4.45 dd (12.0, 2.4)	4.25 dd (12.0, 6.0) 4.40 dd (12.0, 2.4)
inner- Rha					
1''	5.18 d (1.6)	5.17 d (2.0)	5.17 d (1.8)	5.18 d (2.0)	5.15 d (2.0)
2''	3.91 dd (3.2, 1.6)	3.94 dd (3.2, 2.0)	3.94 m	3.94 dd (3.2, 2.0)	3.94 dd (3.2, 2.0)
3''	3.58 m	3.70 dd (9.6, 3.2)	3.70 dd (9.6, 3.6)	3.70 dd (9.6, 3.2)	3.70 dd (9.6, 3.2)
4''	3.29 t (9.6)	3.40 t (9.6)	3.39 t (9.6)	3.39 t (9.6)	3.39 t (9.6)
5''	3.56 m	4.00 dd (9.6, 6.4)	4.00 m	3.99 dd (9.6, 6.4)	3.99 dd (9.6, 6.4)
6''	1.08 d (6.4)	1.25 d (6.4)	1.24 d (6.6)	1.25 d (6.4)	1.24 d (6.4)
outer- Rha					
1'''					
2'''					
3'''					
4'''					
5'''					
6'''					

Table 1. Cont.

No	1 ^b	2 ^b	3 ^c	4a ^b	4b ^b
Ester					
2 ^{'''}	7.05 d (2.0)	7.45 d (8.8)	7.46 d (8.4)	7.46 d (8.8)	7.64 d (8.8)
3 ^{'''}		6.81 d (8.8)	6.80 d (8.4)	6.81 d (8.8)	6.76 d (8.8)
5 ^{'''}	6.77 d (8.0)	6.81 d (8.8)	6.80 d (8.4)	6.81 d (8.8)	6.76 d (8.8)
6 ^{'''}	6.95 dd (8.0, 2.0)	7.45 d (8.8)	7.46 d (8.4)	7.46 d (8.8)	7.64 d (8.8)
7 ^{'''}	7.58 d (16.0)	7.64 d (16.0)	7.64 d (16.2)	7.64 d (16.0)	6.87 d (12.8)
8 ^{'''}	6.27 d (16.0)	6.33 d (16.0)	6.33 d (16.2)	6.34 d (16.0)	5.78 d (12.8)
No	5 ^b	6 ^b	7 ^b	8a ^b	8b ^b
1	5.19 dd (10.8, 1.2) 5.22 dd (17.6, 1.2)	5.23 dd (10.8, 1.6) 5.25 dd (17.6, 1.6)	5.22 dd (10.8, 1.6) 5.24 dd (17.6, 1.6)	4.27 d (8.0)	4.27 d (8.0)
2	5.90 dd (17.6, 10.8)	5.93 dd (17.6, 10.8)	5.92 dd (17.6, 10.8)	5.41 t (8.0)	5.41 t (8.0)
4	2.36 d (7.2)	1.58 m 1.62 m	1.58 m 1.62 m	2.76 d (10.2)	2.76 d (10.2)
5	5.64 dt (16.0, 7.2)	2.05 m	2.04 m	5.55 m	5.55 m
6	5.40 d (16.0)	5.10 m	5.10 m	5.44 d (15.6)	5.44 d (15.6)
8	1.20 s	1.67 s	1.67 s	1.23 s	1.23 s
9	1.20 s	1.60 s	1.60 s	1.23 s	1.23 s
10	1.33 s	1.39 s	1.38 s	1.65 s	1.65 s
7-OCH ₃	3.09 s			3.12 s	3.12 s
Glc					
1'	4.41 d (8.0)	4.44 d (7.6)	4.41 d (8.0)	4.31 d (8.0)	4.27 d (8.0)
2'	3.31 m	3.37 m	3.37 m	3.30 m	3.28 m
3'	3.50 t (8.8)	3.77 t (9.6)	3.77 t (9.6)	3.51 m	3.46 m
4'	3.35 m	4.91 t (9.6)	4.86 t (9.6)	3.37 m	3.33 m
5'	3.49 m	3.46 m	3.46 m	3.51 m	3.47 m
6'	4.32 dd (12.0, 7.2) 4.45 dd (12.0, 2.0)	3.50 m 3.57 m	3.50 m 3.57 m	4.35 dd (12.0, 6.0) 4.50 dd (12.0, 2.0)	4.31 dd (12.0, 6.0) 4.48 dd (12.0, 2.0)
inner- Rha					
1''	5.17 d (2.0)	5.19 d (2.0)	5.29 d (2.0)	5.17 d (2.0)	5.16 d (2.0)
2''	3.94 dd (3.6, 2.0)	3.86 dd (3.2, 2.0)	3.82 dd (3.2, 2.0)	3.94 m	3.92 m
3''	3.70 dd (9.6, 3.6)	3.68 dd (9.6, 3.2)	3.68 dd (9.6, 3.2)	3.70 dd (9.6, 3.2)	3.68 dd (9.6, 3.2)
4''	3.40 t (9.6)	3.39 m	3.45 m	3.40 m	3.40 m
5''	4.00 dd (9.6, 6.4)	3.59 m	3.60 m	4.00 dd (9.6, 6.4)	4.00 dd (9.6, 6.4)
6''	1.25 d (6.4)	1.08 d (6.0)	1.21 d (6.4)	1.24 d (6.4)	1.23 d (6.4)
outer- Rha					
1 ^{'''}		5.04 d (2.0)	5.13 d (2.0)		
2 ^{'''}		3.90 dd (3.2, 2.0)	3.82 dd (3.2, 2.0)		
3 ^{'''}		3.51 m	3.51 m		
4 ^{'''}		3.32 m	3.34 m		
5 ^{'''}		3.46 m	3.46 m		
6 ^{'''}		1.04 d (6.0)	1.21 d (6.4)		
Ester					
2 ^{'''}	7.45 d (8.4)	7.48 d (8.4)	7.72 d (8.4)	7.45 d (8.4)	7.65 d (8.4)
3 ^{'''}	6.81 d (8.4)	6.82 d (8.4)	6.77 d (8.4)	6.80 d (8.4)	6.75 d (8.4)
5 ^{'''}	6.81 d (8.4)	6.82 d (8.4)	6.77 d (8.4)	6.80 d (8.4)	6.75 d (8.4)
6 ^{'''}	7.45 d (8.4)	7.48 d (8.4)	7.72 d (8.4)	7.45 d (8.4)	7.65 d (8.4)
7 ^{'''}	7.63 d (16.0)	7.66 d (16.0)	6.98 d (12.8)	7.64 d (16.0)	6.87 d (12.8)
8 ^{'''}	6.32 d (16.0)	6.33 d (16.0)	5.76 d (12.8)	6.35 d (16.0)	5.79 d (12.8)

^a Coupling constants (*J* values in Hz) are shown in parentheses. ^b At 400 MHz. ^c At 600 MHz.

Table 2. ^{13}C NMR data of compounds 1–8 from *L. robustum* in CD_3OD .

No	1 ^a	2 ^a	3 ^a	4a ^a	4b ^a
1	115.9	115.7	115.8	115.9	115.9
2	144.3	144.3	144.3	144.3	144.3
3	81.6	81.5	81.4	81.5	81.5
4	42.6	42.5	30.2	39.9	39.9
5	23.6	23.6	30.1	26.4	26.4
6	125.7	125.7	76.9	80.1	80.1
7	132.2	132.1	148.7	73.9	73.9
8	25.9	25.8	111.4	24.9	24.9
9	17.7	17.7	17.7	25.8	25.8
10	23.2	23.5	23.5	23.9	23.9
7-OCH ₃					
Glc					
1'	99.4	99.3	99.4	99.4	99.3
2'	76.3	75.7	75.8	75.8	75.8
3'	82.0	84.4	84.4	84.2	84.2
4'	70.7	70.8	70.8	70.7	70.7
5'	75.7	75.0	75.1	75.1	75.0
6'	62.5	65.0	64.9	64.9	62.7
inner-Rha					
1''	103.1	102.8	102.8	102.7	102.4
2''	72.4	72.4	72.4	72.4	72.4
3''	72.0	72.3	72.3	72.3	72.3
4''	73.8	74.0	74.0	74.0	74.0
5''	70.4	70.0	70.0	70.0	70.0
6''	18.5	17.9	17.9	17.9	17.9
outer-Rha					
1'''					
2'''					
3'''					
4'''					
5'''					
6'''					
Ester					
1''''	127.6	127.1	126.9	127.1	127.6
2''''	115.2	131.1	131.2	131.2	133.8
3''''	146.8	116.9	117.0	116.9	115.9
4''''	149.8	161.5	161.9	161.4	160.2
5''''	116.5	116.9	117.0	116.9	115.9
6''''	123.2	131.1	131.2	131.2	133.8
7''''	148.0	146.7	148.7	146.8	145.3
8''''	114.7	115.0	114.8	115.0	116.2
CO	168.3	169.0	169.0	169.0	168.1
No	5 ^a	6 ^b	7 ^b	8a ^a	8b ^a
1	116.0	115.9	115.9	66.3	66.3
2	144.0	144.3	144.3	122.3	122.3
3	81.2	81.6	81.6	140.9	140.9
4	45.5	42.6	42.6	43.5	43.5
5	127.4	23.6	23.7	129.3	129.3
6	139.2	125.7	125.7	138.1	138.1
7	76.5	132.2	132.2	76.4	76.4
8	26.1	25.9	25.9	26.2	26.2
9	26.1	17.7	17.7	26.2	26.2
10	23.5	23.2	23.1	16.6	16.6

Table 2. Cont.

No	5 ^a	6 ^b	7 ^b	8a ^a	8b ^a
7-OCH ₃	50.7			50.6	50.6
Glc					
1'	99.3	99.4	99.4	102.6	102.6
2'	75.8	76.3	76.5	75.6	75.6
3'	84.2	81.9	79.8	84.0	84.0
4'	70.8	70.6	70.4	70.5	70.4
5'	75.0	75.7	75.6	75.5	75.4
6'	64.9	62.4	62.5	64.7	64.5
inner-Rha					
1''	102.8	102.7	101.9	102.7	102.8
2''	72.4	72.7	72.9	72.4	72.4
3''	72.3	72.9	73.0	72.2	72.2
4''	74.0	81.7	80.6	74.0	74.0
5''	70.0	68.9	68.6	70.0	70.3
6''	17.9	19.2	18.9	17.9	17.9
outer-Rha					
1'''		103.5	103.2		
2'''		72.3	72.3		
3'''		72.3	72.3		
4'''		73.8	73.9		
5'''		70.3	70.3		
6'''		17.7	17.8		
Ester					
1''''	127.1	127.0	127.5	126.9	127.5
2''''	131.2	131.4	134.3	131.2	133.8
3''''	116.9	117.0	116.0	117.0	116.0
4''''	161.4	161.5	160.3	161.7	160.3
5''''	116.9	117.0	116.0	117.0	116.0
6''''	131.2	131.4	134.3	131.2	133.8
7''''	146.7	147.5	147.4	146.9	145.3
8''''	115.0	114.8	115.8	114.8	116.2
CO	168.9	168.2	166.9	169.1	168.1

^a At 100 MHz. ^b At 150 MHz.

Compound 4: white amorphous powder. $[\alpha]_D^{23}$ -20.9 (*c* 0.31, MeOH); UV (MeOH) λ_{\max} (log ϵ): 208 (3.9), 229 (3.9), 315 (4.4) nm; IR (film) ν_{\max} : 3369, 2924, 2854, 1695, 1632, 1604, 1515, 1448, 1262, 1170, 833 cm^{-1} ; ¹H NMR (CD₃OD, 400 MHz) data, see Table 1; ¹³C NMR (CD₃OD, 100 MHz) data, see Table 2; HRESIMS *m/z* 665.2784 [M + Na]⁺ (calculated for C₃₁H₄₆NaO₁₄, 665.2785).

Compound 5: white amorphous powder. $[\alpha]_D^{23}$ -29.3 (*c* 0.16, MeOH); UV (MeOH) λ_{\max} (log ϵ): 209 (3.9), 228 (3.9), 315 (4.4) nm; IR (film) ν_{\max} : 3375, 2926, 1694, 1632, 1605, 1515, 1377, 1262, 1169, 1038, 833 cm^{-1} ; ¹H NMR (CD₃OD, 400 MHz) data, see Table 1; ¹³C NMR (CD₃OD, 100 MHz) data, see Table 2; HRESIMS *m/z* 661.2833 [M + Na]⁺ (calculated for C₃₂H₄₆NaO₁₃, 661.2836).

Compound 6: white amorphous powder. $[\alpha]_D^{23}$ -71.0 (*c* 0.35, MeOH); UV (MeOH) λ_{\max} (log ϵ): 209 (3.9), 230 (3.9), 313 (4.4) nm; IR (film) ν_{\max} : 3410, 2973, 1696, 1604, 1515, 1381, 1260, 1168, 1046, 834 cm^{-1} ; ¹H NMR (CD₃OD, 400 MHz) data, see Table 1; ¹³C NMR (CD₃OD, 150 MHz) data, see Table 2; HRESIMS *m/z* 777.3312 [M + Na]⁺ (calculated for C₃₇H₅₄NaO₁₆, 777.3310).

Compound 7: white amorphous powder. $[\alpha]_D^{23}$ -71.0 (*c* 0.35, MeOH); UV (MeOH) λ_{\max} (log ϵ): 208 (3.9), 230 (3.9), 316 (4.4) nm; IR (film) ν_{\max} : 3410, 2973, 1696, 1604, 1515, 1381, 1260, 1168, 1046, 834 cm^{-1} ; ¹H NMR (CD₃OD, 400 MHz) data, see Table 1; ¹³C NMR (CD₃OD, 150 MHz) data, see Table 2; HRESIMS *m/z* 777.3312 [M + Na]⁺ (calculated for C₃₇H₅₄NaO₁₆, 777.3310).

Compound **8**: white amorphous powder. $[\alpha]_D^{23}$ -17.8 (*c* 0.21, MeOH); UV (MeOH) λ_{\max} (log ϵ): 208 (3.9), 230 (3.9), 316 (4.4) nm; IR (film) ν_{\max} : 3391, 2925, 1697, 1632, 1605, 1515, 1446, 1264, 1169, 1041, 834 cm^{-1} ; ^1H NMR (CD_3OD , 400 MHz) data, see Table 1; ^{13}C NMR (CD_3OD , 100 MHz) data, see Table 2; HRESIMS m/z 661.2831 $[\text{M} + \text{Na}]^+$ (calculated for $\text{C}_{32}\text{H}_{46}\text{NaO}_{13}$, 661.2836).

2.4. Acid Hydrolysis of Compounds 1–8

Compounds **1–8** (2 mg) in MeOH (0.1 mL) were added to 1 M H_2SO_4 aqueous solution (2 mL) and heated in 95 °C water bath for 6 h, respectively. The hydrolyzed solution was neutralized with 1 M $\text{Ba}(\text{OH})_2$, filtered and concentrated to a small amount. The monosaccharides in the concentrated solution were identified by TLC with authentic samples, developing with EtOAc-MeOH-HOAc- H_2O (8:1:1:0.7, 2 developments). The R_f values of D-glucose, D-mannose and L-rhamnose were 0.43, 0.46 and 0.73, respectively.

2.5. Enzymatic Hydrolysis of Compounds 1–2

Compound **1** or **2** (20 mg) was hydrolyzed with cellulase (30 mg) in HOAc-NaOAc buffer solution (pH 5.0, 12 mL) at 37 °C for 12 h. The hydrolyzed product was extracted with Et_2O and purified on silica gel column (eluting with CH_2Cl_2), to give (*R*)-linalool and (*S*)-linalool (4:6) confirmed by $[\alpha]_D^{27}$ +3.5 (*c* 0.09, EtOAc) or +2.8 (*c* 0.07, EtOAc).

2.6. Determination of Bioactivities

The inhibitory activities on FAS, α -glucosidase and α -amylase, and the DPPH and ABTS radical scavenging effects of compounds **1–11** were evaluated according to the methods described in the literature [12,18,20], while orlistat, acarbose and L-(+)-ascorbic acid were used as the positive controls, respectively (S1).

2.7. Statistical Analyses

Statistical analyses were carried out on GraphPad Prism 5.01. All samples were measured in triplicate. The IC_{50} (the final concentration of sample needed to inhibit 50% of enzyme activity or scavenge 50% of free radical) was obtained by plotting the inhibition or scavenging percentage of each sample against its concentration. The results are reported as mean \pm standard deviation (SD). Differences of means between groups were analyzed by one-way analysis of variance (ANOVA) on statistical package SPSS 13.0. The differences between groups were believed to be significant when $p < 0.05$.

3. Results and Discussion

3.1. Identification of Compounds 1–11

Compound **1** was analyzed as $\text{C}_{31}\text{H}_{44}\text{O}_{13}$ by HRESIMS (m/z 647.2679 $[\text{M} + \text{Na}]^+$, calculated 647.2680 for $\text{C}_{31}\text{H}_{44}\text{NaO}_{13}$). The ^1H NMR spectrum of **1** (Table 1) revealed the following signals: (1) a 3,4-disubstituted phenyl at δ_{H} 7.05 (1H, d, $J = 2.0$ Hz), 6.95 (1H, dd, $J = 8.0, 2.0$ Hz) and 6.77 (1H, d, $J = 8.0$ Hz); (2) a trans double bond at δ_{H} 7.58 and 6.27 (1H each, d, $J = 16.0$ Hz); (3) a monosubstituted double bond at δ_{H} 5.22 (1H, dd, $J = 10.8, 1.2$ Hz), 5.26 (1H, dd, $J = 17.6, 1.2$ Hz) and 5.93 (1H, dd, $J = 17.6, 10.8$ Hz); (4) an olefinic proton at δ_{H} 5.10 (1H, tt, $J = 7.2, 1.6$ Hz); (5) two anomeric protons at δ_{H} 4.43 (1H, d, $J = 8.0$ Hz) and 5.18 (1H, d, $J = 1.6$ Hz); (6) two methylene groups at δ_{H} 2.04 (2H, m), 1.58, 1.62 (1H each, m), and four methyl groups at δ_{H} 1.67, 1.60, 1.39 (3H each, s), and 1.08 (3H, d, $J = 6.4$ Hz). The ^{13}C NMR spectrum of **1** (Table 2) showed a carbonyl at δ_{C} 168.3, three double bonds at δ_{C} 114.7–148.0, a benzene ring at δ_{C} 115.2–149.8, two anomeric carbons at δ_{C} 99.4 and 103.1, nine sugar carbons at δ_{C} 62.5–82.0, a quaternary carbon at δ_{C} 81.6, two methylene groups at δ_{C} 23.6 and 42.6, and four methyl groups at δ_{C} 17.7–25.9. The above ^1H and ^{13}C NMR features of **1** were related closely to those of linaloyl-(3-*O*- α -L-rhamnopyranosyl)-(4-*O*-*trans*-*p*-coumaroyl)- β -D-glucopyranoside (lipidoside B-III) [21], except that the 4-substituted phenyl in lipidoside B-III was replaced by the 3,4-disubstituted phenyl in **1**. The acid hydrolysis experiment of **1** gave D-glucose and L-rhamnose identified by TLC.

Furthermore, the HMBC experiment of **1** (Figure 2) displayed the long-distance correlations: between δ_{H} 4.33 (H-1' of glucosyl) and δ_{C} 81.6 (C-3 of aglycone), between δ_{H} 5.18 (H-1'' of rhamnosyl) and δ_{C} 82.0 (C-3' of glucosyl), between δ_{H} 7.58 (H-7''' of caffeoyl) and δ_{C} 127.6 (C-1''' of caffeoyl), and between δ_{H} 4.89 (H-4' of glucosyl) and δ_{C} 168.3 (carbonyl of caffeoyl). In addition, the enzymatic hydrolysis experiment of **1** gave (*R*)-linalool and (*S*)-linalool (4:6). The ^1H and ^{13}C NMR signals of **1** were assigned by ^1H - ^1H COSY, HSQC and HMBC experiments (Figure S1). Based on the above evidence, compound **1** was characterized as a mixture (*R*:*S* = 4:6) of 3(*R*)- and 3(*S*)-linaloyl-(3-*O*- α -L-rhamnopyranosyl)-(4-*O*-*trans*-caffeoyl)-*O*- β -D-glucopyranoside. It is a novel monoterpenoid glycoside, named ligurobustoside T.

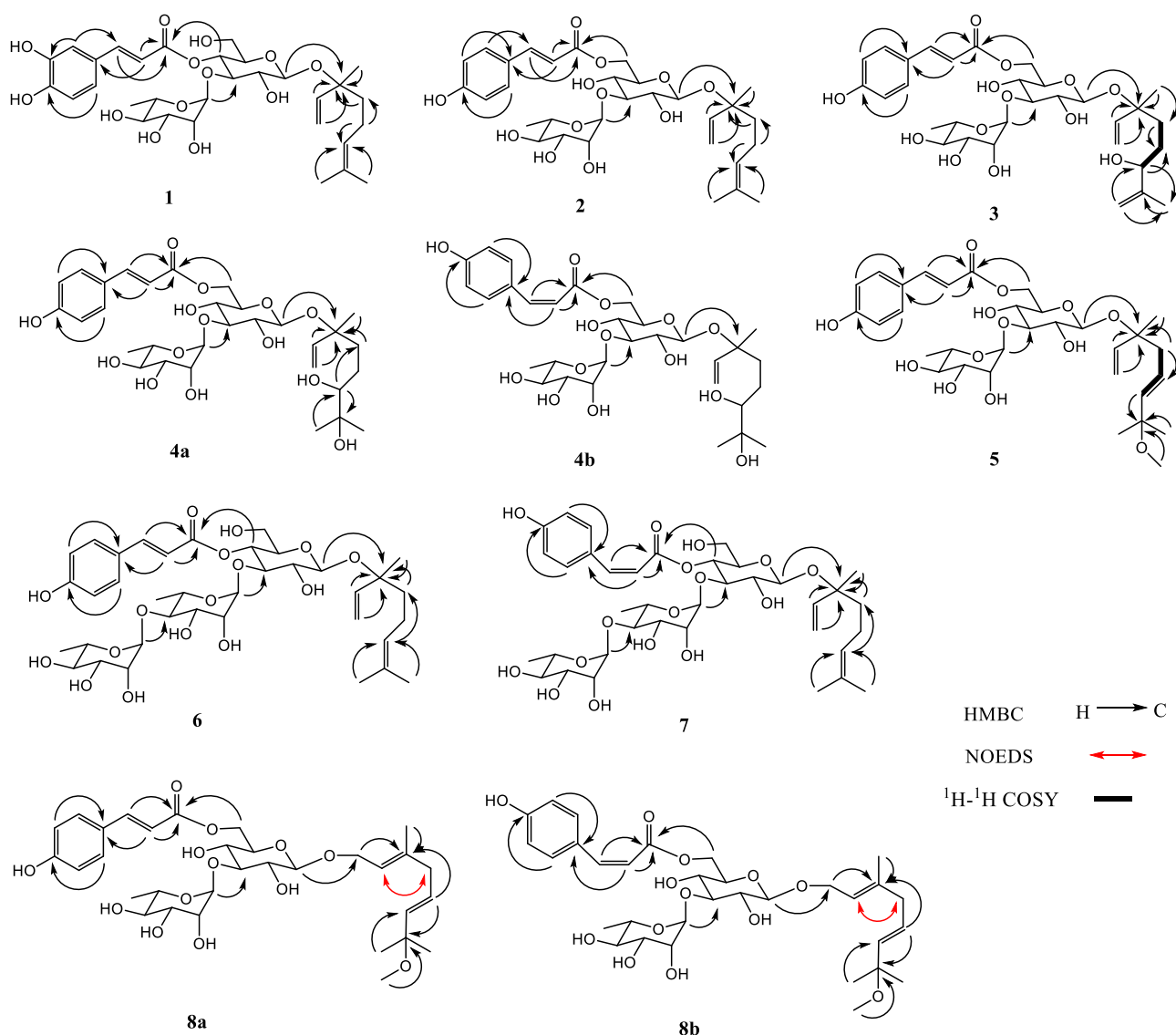


Figure 2. Key HMBC, ^1H - ^1H COSY and NOEDS correlations of compounds 1–8.

Compound **2** was determined as $\text{C}_{31}\text{H}_{44}\text{O}_{12}$ by HRESIMS (m/z 631.2728 [$\text{M} + \text{Na}$] $^+$, calculated 631.2730 for $\text{C}_{31}\text{H}_{44}\text{NaO}_{12}$). The ^1H and ^{13}C NMR data of **2** (Tables 1 and 2) were similar to those of **1**, except the 4-*O*-*trans*-caffeoyl in **1** was replaced by a *trans*-*p*-coumaroyl [δ_{H} 6.81, 7.45 (2H each, d, $J = 8.8$ Hz)] at a different position in **2**. The acid hydrolysis experiment of **2** gave D-glucose and L-rhamnose identified by TLC. The HMBC experiment of **2** (Figure 2) showed the long-distance correlations: between δ_{H} 4.39 (H-1' of glucosyl) and δ_{C} 81.5 (C-3 of aglycone), between δ_{H} 5.17 (H-1'' of rhamnosyl) and δ_{C} 84.4 (C-3' of glucosyl), and between δ_{H} 4.30, 4.45 (H-6' of glucosyl) and δ_{C} 169.0

(carbonyl of coumaroyl). Additionally, the enzymatic hydrolysis experiment of **2** gave (*R*)-linalool and (*S*)-linalool (4:6). The ^1H and ^{13}C NMR signals of **2** were assigned by ^1H - ^1H COSY, HSQC and HMBC experiments (Figure S2). Thus, compound **2** was confirmed as a mixture (*R*:*S* = 4:6) of 3(*R*)- and 3(*S*)-linaloyl-(3-*O*- α -L-rhamnopyranosyl)-(6-*O*-*trans*-*p*-coumaroyl)-*O*- β -D-glucopyranoside, which is a new monoterpenoid glycoside and named ligurobustoside T_1 .

Compound **3** was analyzed as $\text{C}_{31}\text{H}_{44}\text{O}_{13}$ by HRESIMS (m/z 647.2680 [$\text{M} + \text{Na}$] $^+$, calculated 647.2680 for $\text{C}_{31}\text{H}_{44}\text{NaO}_{13}$). The ^1H and ^{13}C NMR data of **3** (Tables 1 and 2) are similar to those of **2** except for some data of the aglycone. The HSQC experiment of **3** displayed the correlations between δ_{H} 4.78 (H-8a of aglycone), 4.88 (H-8b of aglycone) and δ_{C} 111.4 (C-8 of aglycone), meaning that the C-6 double bond in **2** was replaced by the C-7 double bond in **3**. The ^1H - ^1H COSY experiment of **3** (Figure 2) displayed the correlations between δ_{H} 1.22 (H-4 of aglycone), 3.95 (H-6 of aglycone) and δ_{H} 1.60 (H-5 of aglycone), meaning that a hydroxyl was linked at C-6 in **3**. Thus, the aglycone of **3** was 3,7-dimethyl-octa-1,7-diene-3,6-diol. The acid hydrolysis experiment of **3** gave D-glucose and L-rhamnose identified by TLC. The HMBC experiment of **3** (Figure 2) displayed the long-distance correlations: between δ_{H} 4.38 (H-1' of glucosyl) and δ_{C} 81.4 (C-3 of aglycone), between δ_{H} 5.17 (H-1'' of rhamnosyl) and δ_{C} 84.4 (C-3' of glucosyl), and between δ_{H} 4.30, 4.45 (H-6' of glucosyl) and δ_{C} 169.0 (carbonyl of coumaroyl). The ^1H and ^{13}C NMR signals of **3** were assigned by ^1H - ^1H COSY, HSQC and HMBC experiments (Figure S3). Therefore, compound **3** was determined to be 3-(3,6-dihydroxy-3,7-dimethyl-octa-1,7-dienyl)-(3-*O*- α -L-rhamnopyranosyl)-(6-*O*-*trans*-*p*-coumaroyl)-*O*- β -D-glucopyranoside. It is a novel monoterpenoid glycoside named ligurobustoside T_2 .

Compound **4** was analyzed as $\text{C}_{31}\text{H}_{46}\text{O}_{14}$ by HRESIMS (m/z 665.2784 [$\text{M} + \text{Na}$] $^+$, calculated 665.2785 for $\text{C}_{31}\text{H}_{46}\text{NaO}_{14}$). The NMR spectra of **4** showed two stereoisomers **4a** and **4b** (2:1). The ^1H NMR spectrum of **4a** (Table 1) displayed the following signals: (1) a 4-substituted phenyl at δ_{H} 6.81, 7.46 (2H each, d, $J = 8.8$ Hz); (2) a *trans* double bond at δ_{H} 6.34, 7.64 (1H each, d, $J = 16.0$ Hz); (3) a monosubstituted double bond at δ_{H} 5.19 (1H, dd, $J = 10.8, 2.0$ Hz), 5.24 (1H, dd, $J = 18.0, 2.0$ Hz) and 5.92 (1H, dd, $J = 18.0, 10.8$ Hz); (4) two anomeric protons at δ_{H} 4.41 (1H, d, $J = 8.0$ Hz), 5.18 (1H, d, $J = 2.0$ Hz); (5) a methenyl at δ_{H} 3.21 (1H, dd, $J = 10.4, 2.0$ Hz); (6) two methylene groups at δ_{H} 1.32–1.90 (4H, m); (7) four methyl groups at δ_{H} 1.11, 1.14, 1.36 (3H each, s), 1.25 (3H, d, $J = 6.4$ Hz). The ^{13}C NMR spectrum of **4a** (Table 2) revealed a carbonyl at δ_{C} 169.0, two double bonds at δ_{C} 115.0–146.8, a 4-substituted phenyl at δ_{C} 116.9–161.4, two anomeric carbons at δ_{C} 99.4 and 102.7, nine sugar carbons at δ_{C} 64.9–84.2, two quaternary carbons at δ_{C} 73.9 and 81.5, a methenyl at δ_{C} 80.1, two methylene groups at δ_{C} 26.4 and 39.9, and four methyl groups at δ_{C} 17.9–25.8. The above ^1H and ^{13}C NMR data of **4a** were similar to those of 3-(6,7-dihydroxy-3,7-dimethyloct-1-enyl)-(3-*O*- α -L-rhamnopyranosyl)-(4-*O*-*trans*-*p*-coumaroyl)-*O*- β -D-glucopyranoside (lipedoside B-VI) [21], except the *trans*-*p*-coumaroyl was linked at different positions. The acid hydrolysis experiment of **4** gave D-glucose and L-rhamnose identified by TLC. The HMBC experiment of **4a** (Figure 2) displayed the long-distance correlations: between δ_{H} 4.41 (H-1' of glucosyl) and δ_{C} 81.5 (C-3 of aglycone), between δ_{H} 5.18 (H-1'' of rhamnosyl) and δ_{C} 84.2 (C-3' of glucosyl), and between δ_{H} 4.30, 4.45 (H-6' of glucosyl) and δ_{C} 169.0 (carbonyl of coumaroyl). The ^1H and ^{13}C NMR signals of **4** were assigned by ^1H - ^1H COSY, HSQC and HMBC experiments (Figure S4). So, **4a** was identified as 3-(3,6,7-trihydroxy-3,7-dimethyloct-1-enyl)-(3-*O*- α -L-rhamnopyranosyl)-(6-*O*-*trans*-*p*-coumaroyl)-*O*- β -D-glucopyranoside.

The NMR data of **4b** (Tables 1 and 2) are similar to those of **4a**, except the *trans*-*p*-coumaroyl in **4a** was replaced by the *cis*-*p*-coumaroyl (δ_{H} 6.87, 5.78 (1H each, d, $J = 12.8$ Hz, H-7''', H-8''')) in **4b**. The HMBC experiment of **4b** (Figure 2) showed the long-distance correlations: between δ_{H} 4.36 (H-1' of glucosyl) and δ_{C} 81.5 (C-3 of aglycone), between δ_{H} 5.15 (H-1'' of rhamnosyl) and δ_{C} 84.2 (C-3' of glucosyl), and between δ_{H} 4.25, 4.40 (H-6' of glucosyl) and δ_{C} 168.1 (carbonyl of coumaroyl). So, **4b** was identified as 3-(3,6,7-trihydroxy-3,7-dimethyloct-1-enyl)-(3-*O*- α -L-rhamnopyranosyl)-(6-*O*-*cis*-*p*-

cou-maroyl)-*O*- β -D-glucopyranoside. In conclusion, compound **4** is a mixture of novel monoterpenoid glycosides **4a** and **4b**, named ligurobustoside T₃₋₄.

Compound **5** was analyzed as C₃₂H₄₆O₁₃ by HRESIMS (m/z 661.2833 [M + Na]⁺, calculated 661.2836 for C₃₂H₄₆NaO₁₃). The ¹H and ¹³C NMR data of **5** (Tables 1 and 2) are similar to those of **2** except for some data of the aglycone. The ¹H-¹H COSY experiment of **5** (Figure 2) displayed the correlations between δ_H 2.36 (2H, d, $J = 7.2$ Hz, H-4 of aglycone), 5.40 (1H, d, $J = 16.0$ Hz, H-6 of aglycone) and δ_H 5.64 (1H, dt, $J = 16.0, 7.2$ Hz, H-5 of aglycone), meaning that the C-6 double bond in **2** was replaced by the C-5(E) double bond in **5**. The HMBC experiment of **5** (Figure 2) displayed the correlation between δ_H 3.09 (OCH₃) and δ_C 76.5 (C-7 of aglycone). Hence, the aglycone of **5** was (5E)-7-methoxy-3,7-dimethyl-octa-1,5-dien-3-ol. The acid hydrolysis experiment of **5** gave D-glucose and L-rhamnose identified by TLC. The HMBC experiment of **5** (Figure 2) displayed the long-distance correlations: between δ_H 4.41 (H-1' of glucosyl) and δ_C 81.2 (C-3 of aglycone), between δ_H 5.17 (H-1'' of rhamnosyl) and δ_C 84.2 (C-3' of glucosyl), and between δ_H 4.32, 4.45 (H-6' of glucosyl) and δ_C 168.9 (carbonyl of coumaroyl). The ¹H and ¹³C NMR signals of **5** were assigned by ¹H-¹H COSY, HSQC and HMBC experiments (Figure S5). Therefore, compound **5** was determined to be (5E)-3-(3-hydroxy-7-methoxy-3,7-dimethyl-octa-1,5-dienyl)-(3-*O*- α -L-rhamnopyranosyl)-(6-*O*-*trans*-*p*-coumaroyl)-*O*- β -D-glucopyranoside. It is a novel monoterpenoid glycoside, named ligurobustoside T₅.

Compound **6** was determined as C₃₇H₅₄O₁₆ by HRESIMS (m/z 777.3312 [M + Na]⁺, calculated 777.3310 for C₃₇H₅₄NaO₁₆). The ¹H and ¹³C NMR data of **6** (Tables 1 and 2) are similar to those of lipedoside B-III [21], except there was another rhamnosyl in **6**. The acid hydrolysis experiment of **6** yielded D-glucose and L-rhamnose identified by TLC. The HMBC experiment of **6** (Figure 2) showed the long-distance correlations: between δ_H 4.44 (H-1' of glucosyl) and δ_C 81.6 (C-3 of aglycone), between δ_H 5.19 (H-1'' of inner rhamnosyl) and δ_C 81.9 (C-3' of glucosyl), between δ_H 5.04 (H-1''' of outer rhamnosyl) and δ_C 81.7 (C-4'' of inner rhamnosyl), and between δ_H 4.91 (H-4' of glucosyl) and δ_C 168.2 (carbonyl of coumaroyl). The ¹H and ¹³C NMR signals of **6** were assigned by ¹H-¹H COSY, HSQC and HMBC experiments (Figure S6). Thus, compound **6** was confirmed as linaloyl-[3-*O*- α -L-rhamnopyranosyl-(1 \rightarrow 4)- α -L-rhamnopyranosyl]-(4-*O*-*trans*-*p*-coumaroyl)-*O*- β -D-glucopyranoside, which is a new monoterpenoid glycoside and named ligurobustoside T₆.

Compound **7** was determined as C₃₇H₅₄O₁₆ by HRESIMS (m/z 777.3312 [M + Na]⁺, calculated 777.3310 for C₃₇H₅₄NaO₁₆). The ¹H and ¹³C NMR data of **7** (Tables 1 and 2) are related closely to those of **6**, except the *trans*-*p*-coumaroyl (δ_H 7.66, 6.33 (1H each, d, $J = 16.0$ Hz, H-7''', H-8''')) in **6** was replaced by the *cis*-*p*-coumaroyl (δ_H 6.98, 5.76 (1H each, d, $J = 12.8$ Hz, H-7''', H-8''')) in **7**. The acid hydrolysis experiment of **7** yielded D-glucose and L-rhamnose identified by TLC. The HMBC experiment of **7** (Figure 2) showed the long-distance correlations: between δ_H 4.41 (H-1' of glucosyl) and δ_C 81.6 (C-3 of aglycone), between δ_H 5.29 (H-1'' of inner rhamnosyl) and δ_C 79.8 (C-3' of glucosyl), between δ_H 5.13 (H-1''' of outer rhamnosyl) and δ_C 80.6 (C-4'' of inner rhamnosyl), and between δ_H 4.86 (H-4' of glucosyl) and δ_C 166.9 (carbonyl of coumaroyl). The ¹H and ¹³C NMR signals of **7** were assigned by ¹H-¹H COSY, HSQC and HMBC experiments (Figure S7). Thus, compound **7** was identified as linaloyl-[3-*O*- α -L-rhamnopyranosyl-(1 \rightarrow 4)- α -L-rhamnopyranosyl]-(4-*O*-*cis*-*p*-coumaroyl)-*O*- β -D-glucopyranoside. It is a new monoterpenoid glycoside, named ligurobustoside T₇.

Compound **8** was analyzed as C₃₂H₄₆O₁₃ by HRESIMS (m/z 661.2831 [M + Na]⁺, calculated 661.2836 for C₃₂H₄₆NaO₁₃). The NMR spectra of **8** exhibited two stereoisomers **8a** and **8b** (2:1). The ¹H NMR spectrum of **8a** (Table 1) displayed the following signals: (1) a 4-substituted phenyl at δ_H 6.80, 7.45 (2H each, d, $J = 8.4$ Hz); (2) two *trans* double bonds at δ_H 6.35, 7.64 (1H each, d, $J = 16.0$ Hz), 5.44 (1H, d, $J = 15.6$ Hz), 5.55 (1H, m); (3) an olefinic proton at δ_H 5.41 (1H, t, $J = 8.0$ Hz); (4) two anomeric protons at δ_H 4.31 (1H, d, $J = 8.0$ Hz), 5.17 (1H, d, $J = 2.0$ Hz); (5) two methylene groups at δ_H 4.27 (2H, d, $J = 8.0$ Hz), 2.76 (2H, d, $J = 10.2$ Hz); (6) four methyl groups at δ_H 1.23, 1.23, 1.65 (3H each, s), 1.24 (3H,

d, $J = 6.4$ Hz); and (7) a methoxy at $\delta_{\text{H}} 3.12$ (3H, s). The ^{13}C NMR spectrum of **8a** (Table 2) revealed a carbonyl at $\delta_{\text{C}} 169.1$, three double bonds at $\delta_{\text{C}} 114.8$ – 146.9 , a 4-substituted phenyl at $\delta_{\text{C}} 117.0$ – 161.7 , two anomeric carbons at $\delta_{\text{C}} 102.6$ and 102.7 , nine sugar carbons at $\delta_{\text{C}} 64.7$ – 84.0 , a quaternary carbon at $\delta_{\text{C}} 76.4$, two methylene groups at $\delta_{\text{C}} 66.3$, 43.5 , a methoxy at $\delta_{\text{C}} 50.6$, and four methyl groups at $\delta_{\text{C}} 16.6$ – 26.2 . The above ^1H and ^{13}C NMR data of **8a** were similar to those of (2*E*,5*E*)-1-(1,7-dihydroxy-3,7-dimethyl-2,5-octa-dienyl)-(3-*O*- α -L-rhamnopyranosyl)-(4-*O*-*trans*-*p*-coumaroyl)-*O*- β -D-glucopyranoside (ligurobustoside I) [8], except the *trans*-*p*-coumaroyl was linked at different positions, and there was another methyl in **8a**. The HMBC experiment of **8a** (Figure 2) showed the correlation between $\delta_{\text{H}} 3.12$ (OCH₃) and $\delta_{\text{C}} 76.4$ (C-7 of aglycone). The NOEDS experiment of **8a** (Figure 2) displayed the correlation between $\delta_{\text{H}} 5.41$ (H-2 of aglycone) and $\delta_{\text{H}} 2.76$ (H-4 of aglycone). Therefore, the aglycone of **8a** was (2*E*,5*E*)-7-methoxy-3,7-dimethyl-octa-2,5-dien-1-ol. The acid hydrolysis experiment of **8** gave D-glucose and L-rhamnose identified by TLC. The HMBC experiment of **8a** (Figure 2) displayed the long-distance correlations: between $\delta_{\text{H}} 4.31$ (H-1' of glucosyl) and $\delta_{\text{C}} 66.3$ (C-1 of aglycone), between $\delta_{\text{H}} 5.17$ (H-1'' of rhamnosyl) and $\delta_{\text{C}} 84.0$ (C-3' of glucosyl), and between $\delta_{\text{H}} 4.35$, 4.50 (H-6' of glucosyl) and $\delta_{\text{C}} 169.1$ (carbonyl of coumaroyl). The ^1H and ^{13}C NMR signals of **8** were assigned by ^1H - ^1H COSY, HSQC and HMBC experiments (Figure S8). Consequently, the structure of **8a** was determined to be (2*E*,5*E*)-1-(1-hydroxy-7-methoxy-3,7-dimethyl-octa-2,5-dienyl)-(3-*O*- α -L-rhamnopyranosyl)-(6-*O*-*trans*-*p*-coumaroyl)-*O*- β -D-glucopyranoside.

The NMR data of **8b** (Tables 1 and 2) are similar to those of **8a**, except the *trans*-*p*-coumaroyl in **8a** was replaced by the *cis*-*p*-coumaroyl ($\delta_{\text{H}} 6.87$, 5.79 (1H each, d, $J = 12.8$ Hz, H-7''', H-8''')) in **8b**. The HMBC experiment of **8b** (Figure 2) displayed the long-distance correlations: between $\delta_{\text{H}} 4.27$ (H-1' of glucosyl) and $\delta_{\text{C}} 66.3$ (C-1 of aglycone), between $\delta_{\text{H}} 5.16$ (H-1'' of rhamnosyl) and $\delta_{\text{C}} 84.0$ (C-3' of glucosyl), and between $\delta_{\text{H}} 4.31$, 4.48 (H-6' of glucosyl) and $\delta_{\text{C}} 168.1$ (carbonyl of coumaroyl). So, **8b** was identified as (2*E*,5*E*)-1-(1-hydroxy-7-methoxy-3,7-dimethyl-octa-2,5-dienyl)-(3-*O*- α -L-rhamnopyranosyl)-(6-*O*-*cis*-*p*-coumaroyl)-*O*- β -D-glucopyranoside. In conclusion, compound **8** is a mixture of novel monoterpenoid glycosides **8a** and **8b**, named ligurobustoside T₈₋₉.

Compounds **9**–**11** (NMR data see Tables S1–S3) were identified as ligurobustosides G (**9a**) and H (**9b**), ligurobustoside C (**10**), ligurobustosides K (**11a**) and L (**11b**), respectively, by direct comparison with published spectral data (^1H , ^{13}C NMR) [8,9].

3.2. The Bioactivities of Compounds 1–11

Compounds **1**–**11** from the leaves of *L. robustum* were tested for the inhibitory activities on FAS, α -glucosidase, α -amylase, and the antioxidant effects. The results of bioactivity assays are shown in Table 3. As shown in Table 3, compound **2** revealed stronger FAS inhibitory activity (IC_{50} : 2.36 ± 0.10 μM) than the positive control orlistat (IC_{50} : 4.46 ± 0.13 μM); compound **2** showed weaker α -glucosidase inhibitory effect than the positive control acarbose; compounds **2**–**6**, **8**, **9** and **11** displayed weaker α -amylase inhibitory effect than the positive control acarbose; compounds **1**, **2**, **5** and **11** exhibited more potent ABTS radical scavenging activity (IC_{50} : 6.91 ± 0.10 – 9.41 ± 0.22 μM) than the positive control L-(+)-ascorbic acid (IC_{50} : 10.06 ± 0.19 μM), while compound **1** displayed weaker DPPH radical scavenging activity (IC_{50} : 19.74 ± 0.23 μM) than L-(+)-ascorbic acid (IC_{50} : 13.66 ± 0.13 μM).

Table 3. The results of bioactivity assays of compounds 1–11 from *L. robustum* ^a.

Compounds	FAS IC ₅₀ (μM) ^b	α-Glucosidase Inhibition at 0.1 mM (%)	α-Amylase Inhibition at 0.1 mM (%)	DPPH IC ₅₀ (μM) ^b	ABTS•• IC ₅₀ (μM) ^b
1	NA ^c	NA	NA	19.74 ± 0.23 b	6.91 ± 0.10 a
2	2.36 ± 0.10 a	48.1 ± 4.3 b	31.5 ± 0.5 b	>250	9.41 ± 0.22 c
3	21.77 ± 0.38 c	27.3 ± 0.3 c	32.5 ± 6.3 b	NA	16.00 ± 0.69 g
4	>100	NA	28.2 ± 3.9 b	NA	9.66 ± 0.17 cd
5	23.71 ± 0.45 d	13.8 ± 2.0 d	35.6 ± 2.0 b	NA	6.93 ± 0.01 a
6	4.78 ± 0.14 b	12.0 ± 1.7 d	26.1 ± 3.0 b	NA	11.30 ± 0.16 e
7	>100	NA	NA	NA	20.21 ± 0.33 j
8	25.83 ± 0.47 e	24.7 ± 3.5 c	31.4 ± 1.9 b	NA	19.50 ± 0.46 i
9	21.67 ± 0.46 c	12.4 ± 5.6 d	29.2 ± 8.4 b	NA	18.66 ± 0.47 h
10	4.68 ± 0.16 b	28.7 ± 2.1 c	NA	NA	15.10 ± 0.10 f
11	61.74 ± 0.45 f	NA	31.3 ± 1.3 b	NA	7.92 ± 0.23 b
Orlistat ^d	4.46 ± 0.13 b				
Acarbose ^d		93.2 ± 0.1 a	51.8 ± 2.5 a		
L-(+)-ascorbic acid ^d				13.66 ± 0.13 a	10.06 ± 0.19 d

^a Data are expressed as mean ± SD (*n* = 3). Means with the same letter are not significantly different (one-way analysis of variance, α = 0.05). ^b IC₅₀: the final concentration of sample needed to inhibit 50% of enzyme activity or scavenge 50% of free radical. ^c NA: no activity. ^d Positive control.

Because FAS is a potential therapeutic target for anti-obesity drugs [17–19], compounds 2, 6 and 10 with strong FAS inhibitory activity might be a part of the constituents with anti-obesity activity in *L. robustum*. In addition, the results suggested that the FAS inhibitory activity would reduce or disappear when the monoterpene unit of glycoside was substituted with hydroxyl, or the *trans-p*-coumaroyl of glycoside was replaced by other groups.

4. Conclusions

In summary, the phytochemical research on the leaves of *L. robustum* resulted in the separation of eleven monoterpenoid glycosides (1–11), including eight new compounds (1–8) identified with spectroscopic method (¹H, ¹³C NMR, ¹H-¹H COSY, HSQC, HMBC, NOEDS, HRESIMS), and physical and chemical methods. The biological study showed that compound 2 revealed stronger FAS inhibitory activity (IC₅₀: 2.36 ± 0.10 μM) than the positive control orlistat (IC₅₀: 4.46 ± 0.13 μM); compounds 1, 2, 5 and 11 displayed more potent ABTS radical scavenging activity (IC₅₀: 6.91 ± 0.10–9.41 ± 0.22 μM) than the positive control L-(+)-ascorbic acid (IC₅₀: 10.06 ± 0.19 μM); compound 2 revealed also moderate α-glucosidase and α-amylase inhibitory activities. This study provided a theoretical basis for the leaves of *L. robustum* as a functional tea to treat obesity.

Supplementary Materials: The following are available online <https://www.mdpi.com/article/10.3390/molecules27123709/s1>. ¹H NMR, ¹³C NMR, ¹H-¹H COSY, HSQC, HMBC, HRESIMS and IR spectra of compounds 1 (Figure S1) and 3–6 (Figures S3–S6); ¹H NMR, ¹³C NMR, HMBC, HRESIMS and IR spectra of compounds 2 (Figure S2) and 7 (Figure S7); ¹H NMR, ¹³C NMR, ¹H-¹H COSY, HSQC, HMBC, NOEDS, HRESIMS and IR spectra of compound 8 (Figure S8); ¹H NMR and ¹³C NMR data of 9–11 (Tables S1–S3); determination of bioactivities (S1).

Author Contributions: Conceptualization, S.-H.L., J.H. and H.-J.Z.; methodology, S.-H.L.; formal analysis, S.-H.L. and Z.-B.Z.; investigation, S.-H.L., H.-J.Z., Z.-B.Z. and C.-Y.Y.; data curation, J.H.; writing—original draft preparation, S.-H.L.; writing review and editing, J.H. and Z.-L.H.; supervision, J.H. and Z.-L.H.; funding acquisition, S.-H.L. All authors have read and agreed to the published version of the manuscript.

Funding: This research was funded by the Guangxi Natural Science Foundation Project (grant number 2020GXNSFAA297129), Guangxi Science and Technology Base and Talents Special Project (grant number Guike AD21075006), and Youjiang Medical University for Nationalities Science Research Project (grant number yy2021sk004).

Institutional Review Board Statement: Not applicable.

Informed Consent Statement: Not applicable.

Data Availability Statement: Not applicable.

Acknowledgments: The authors thank sincerely You Zhou and Fu Su, West China School of Pharmacy, Sichuan University, for the NMR measurements. The authors are grateful to Ming-Hai Tang, State Key Laboratory of Biotherapy, West China Hospital, Sichuan University, for the HRESIMS measurement.

Conflicts of Interest: The authors declare no conflict of interest. The funders had no role in the design of the study; in the collection, analyses, or interpretation of data; in the writing of the manuscript, or in the decision to publish the results.

Sample Availability: Samples of the compounds are not available from the authors.

References

1. He, Z.D.; Lau, K.M.; But, P.P.-H.; Jiang, R.W.; Dong, H.; Ma, S.C.; Fung, K.P.; Ye, W.C.; Sun, H.D. Antioxidative glycosides from the leaves of *Ligustrum robustum*. *J. Nat. Prod.* **2003**, *66*, 851–854. [[CrossRef](#)] [[PubMed](#)]
2. Yang, R.M.; Liu, F.; He, Z.D.; Ji, M.; Chu, X.X.; Kang, Z.Y.; Cai, D.Y.; Gao, N.N. Anti-obesity effect of total phenylpropanoid glycosides from *Ligustrum robustum* Blume in fatty diet-fed mice via up-regulating leptin. *J. Ethnopharmacol.* **2015**, *169*, 459–465. [[CrossRef](#)] [[PubMed](#)]
3. Zhu, F.; Cai, Y.Z.; Sun, M.; Ke, J.X.; Lu, D.Y.; Corke, H. Comparison of major phenolic constituents and in vitro antioxidant activity of diverse kudingcha genotypes from *Ilex kudingcha*, *Ilex cornuta*, and *Ligustrum robustum*. *J. Agric. Food Chem.* **2009**, *57*, 6082–6089. [[CrossRef](#)] [[PubMed](#)]
4. Lau, K.M.; He, Z.D.; Dong, H.; Fung, K.P.; But, P.P.-H. Anti-oxidative, anti-inflammatory and hepato-protective effects of *Ligustrum robustum*. *J. Ethnopharmacol.* **2002**, *83*, 63–71. [[CrossRef](#)]
5. Xie, Z.M.; Zhou, T.; Liao, H.Y.; Ye, Q.; Liu, S.; Qi, L.; Huang, J.; Zuo, H.J.; Pei, X.F. Effects of *Ligustrum robustum* on gut microbes and obesity in rats. *World J. Gastroenterol.* **2015**, *21*, 13042–13054. [[CrossRef](#)]
6. Li, L.; Peng, Y.; Xu, L.J.; Wu-Lan, T.N.; Shi, R.B.; Xiao, P.G. Chemical constituents from *Ligustrum robustum* Bl. *Biochem. Syst. Ecol.* **2010**, *38*, 398–401. [[CrossRef](#)]
7. Li, L.; Peng, Y.; Liu, Y.; Xu, L.J.; Guo, N.; Shi, R.B.; Xiao, P.G. Two new phenethanol glycosides from *Ligustrum robustum*. *Chin. Chem. Lett.* **2011**, *22*, 326–329. [[CrossRef](#)]
8. Tian, J.; Zhang, H.J.; Sun, H.D.; Pan, L.T.; Yao, P.; Chen, D.Y. Monoterpenoid glycosides from *Ligustrum robustum*. *Phytochemistry* **1998**, *48*, 1013–1018. [[CrossRef](#)]
9. Tian, J.; Sun, H.D. New monoterpenoid glycosides from *Ligustrum robustum*. *Chin. J. Appl. Environ. Biol.* **1999**, *5*, 501–506.
10. Yu, Z.L.; Zeng, W.C. Antioxidant, antibrowning, and cytoprotective activities of *Ligustrum robustum* (Roxb.) Blume extract. *J. Food Sci.* **2013**, *78*, 1354–1362.
11. Yu, Z.L.; Gao, H.X.; Zhang, Z.; He, Z.; He, Q.; Jia, L.R.; Zeng, W.C. Inhibitory effects of *Ligustrum robustum* (Roxb.) Blume extract on α -amylase and α -glucosidase. *J. Funct. Foods* **2015**, *19*, 204–213. [[CrossRef](#)]
12. Lu, S.-H.; Zuo, H.-J.; Shi, J.-X.; Li, C.-R.; Li, Y.-H.; Wang, X.; Li, L.-R.; Huang, J. Two new glycosides from the leaves of *Ligustrum robustum* and their antioxidant activities and inhibitory effects on α -glucosidase and α -amylase. *S. Afr. J. Bot.* **2019**, *125*, 521–526. [[CrossRef](#)]
13. Jang, J.H.; Park, J.E.; Han, J.S. Scopoletin inhibits α -glucosidase in vitro and alleviates postprandial hyperglycemia in mice with diabetes. *Eur. J. Pharmacol.* **2018**, *834*, 152–156. [[CrossRef](#)]
14. Sirdah, M.M. Protective and therapeutic effectiveness of taurine in diabetes mellitus: A rationale for antioxidant supplementation. *Diabetes Metab. Syndr. Clin. Res. Rev.* **2015**, *9*, 55–64. [[CrossRef](#)] [[PubMed](#)]
15. Spadiene, A.; Savickiene, N.; Ivanauskas, L.; Jakstas, V.; Skesters, A.; Silova, A.; Rodovicus, H. Antioxidant effects of *Camellia sinensis* L. extract in patients with type 2 diabetes. *J. Food Drug Anal.* **2014**, *22*, 505–511. [[CrossRef](#)]
16. Zemestani, M.; Rafraf, M.; Asghari-Jafarabadi, M. Chamomile tea improves glycemic indices and antioxidants status in patients with type 2 diabetes mellitus. *Nutrition* **2016**, *32*, 66–72. [[CrossRef](#)]
17. Buckley, D.; Duke, G.; Heuer, T.S.; O'Farrell, M.; Wagman, A.S.; McCulloch, W.; Kemble, G. Fatty acid synthase—Modern tumor cell biology insights into a classical oncology target. *Pharmacol. Therapeut.* **2017**, *177*, 23–31. [[CrossRef](#)]
18. Fan, H.J.; Wu, D.; Tian, W.X.; Ma, X.F. Inhibitory effects of tannic acid on fatty acid synthase and 3T3-L1 preadipocyte. *Biochim. Biophys. Acta* **2013**, *1831*, 1260–1266. [[CrossRef](#)]
19. Lu, T.B.; Schubert, C.; Cummings, M.D.; Bignan, G.; Connolly, P.J.; Smans, K.; Ludovici, D.; Parker, M.H.; Meyer, C.; Rocaboy, C.; et al. Design and synthesis of a series of bioavailable fatty acid synthase (FASN) KR domain inhibitors for cancer therapy. *Bioorg. Med. Chem. Lett.* **2018**, *28*, 2159–2164. [[CrossRef](#)]
20. Wu, D.; Ma, X.F.; Tian, W.X. Pomegranate husk extract, punicalagin and ellagic acid inhibit fatty acid synthase and adipogenesis of 3T3-L1 adipocyte. *J. Funct. Foods* **2013**, *5*, 633–641. [[CrossRef](#)]
21. He, Z.D.; Ueda, S.; Akaji, M.; Fujita, T.; Inoue, K.; Yang, C.R. Monoterpenoid and phenylethanoid glycosides from *Ligustrum Pedunculare*. *Phytochemistry* **1994**, *36*, 709–716. [[CrossRef](#)]